

# A relativistic approach for determination of nuclear and neutron star properties in consideration of PREX-II results

Virender Thakur,<sup>1,\*</sup> Raj Kumar,<sup>1,†</sup> Pankaj Kumar,<sup>2</sup> Mukul Kumar,<sup>1</sup> C. Mondal,<sup>3</sup>  
Kaixuan Huang,<sup>4</sup> Jinniu Hu,<sup>4</sup> B.K. Agrawal,<sup>5,‡</sup> and Shashi K. Dhiman<sup>1,6,§</sup>

<sup>1</sup>*Department of Physics, Himachal Pradesh University, Shimla-171005, India*

<sup>2</sup>*Department of Applied Sciences, CGC College of Engineering, Landran, Mohali 140307, India*

<sup>3</sup>*Laboratoire de Physique Corpusculaire, CNRS, ENSICAEN, UMR6534,*

*Université de Caen Normandie, F-14000, Caen Cedex, France*

<sup>4</sup>*School of Physics, Nankai University, Tianjin 300071, China*

<sup>5</sup>*Saha Institute of Nuclear Physics, 1/AF Bidhannagar, Kolkata 700064, India*

<sup>6</sup>*School of Applied Sciences, Himachal Pradesh Technical University, Hamirpur-177001, India*

The bulk properties of nuclear matter and neutron stars with the newly generated relativistic interaction DBHP are investigated which provides an opportunity to modify the coupling parameters keeping in view the finite nuclei, nuclear matter, PREX-II data for neutron skin thickness in <sup>208</sup>Pb and astrophysical constraints. The relativistic interaction has been generated by including all possible self and mixed interactions between  $\sigma$ ,  $\omega$ , and  $\rho$ -meson up to the quartic order satisfying the naturalness behavior of parameters. A covariance analysis is performed to assess the statistical uncertainties on the model parameters and observables of interest along with correlations amongst them. We obtained a value of neutron skin thickness for <sup>208</sup>Pb nucleus  $\Delta r_{np} = 0.24 \pm 0.02$  fm. The maximum gravitational mass of neutron star and radius corresponding to the canonical mass ( $R_{1.4}$ ) come out to be  $2.03 \pm 0.04 M_{\odot}$  and  $13.39 \pm 0.41$  km respectively. The dimensionless tidal deformability,  $\Lambda$  for a neutron star is also analyzed.

## I. INTRODUCTION

Neutron stars (NSs) are highly dense and asymmetric nuclear systems having a central density about 5-6 times the nuclear saturation density [1]. The studies of the NSs proclaim that their internal structure are quite complex as new degrees of freedom like hyperons and quarks may appear in the core. The NS properties like mass, radius, and tidal deformability can be estimated using equations of state (EoSs) obtained within various theoretical models [2–4]. One of such models is based on the relativistic interaction which describes the interaction between nucleons through  $\sigma$ ,  $\omega$  and  $\rho$  mesons. There are several models of relativistic mean field (RMF) effective lagrangian density consisting of nonlinear  $\sigma$ ,  $\omega$ , and  $\rho$  terms and cross terms that have been analyzed for nucleonic and hyperonic matter and confronted with the constraints of nuclear matter properties and astrophysical observations of NS masses [5–9].

The nuclear theory studies [10–12] are mainly focusing on understanding the dense matter in NS. The constraints on EOS at high density are imposed with currently available lower bound on neutron star's maximum mass and radius [13–15]. The precise measurement of masses of millisecond pulsars such as PSR J1614-2230 [16], PSR J0348+0432 [17] show that the maximum mass of the NS should be around  $2 M_{\odot}$ . The recent observations with LIGO and Virgo of GW170817 event [18, 19]

of Binary Neutron Stars merger and the discovery of NS with masses around  $2M_{\odot}$  [16, 17, 20–23] have intensified the interest in these intriguing objects. The analysis of GW170817 has demonstrated the potential of gravitational wave (GW) observations to yield new information relating to the limits on NS tidal deformability. The Lead Radius Experiment (PREX-II) has recently provided a model-independent extraction of neutron skin thickness of <sup>208</sup>Pb as  $\Delta r_{np} = 0.283 \pm 0.071$  fm [24]. The  $\Delta r_{np}$  has been identified as an ideal probe for the density dependence of symmetry energy - a key but poorly known quantity that describes the isospin dependence of the EOS of asymmetric nuclear matter and plays a critical role in various issues in nuclear physics and astrophysics. The neutron skin thickness of the Lead nucleus exhibit a strong positive linear correlation with the slope of symmetry energy parameter ( $L$ ) at saturation density. The parameter  $L$  that determines the density dependence of symmetry energy strongly affects the Mass-Radius relation and tidal deformability ( $\Lambda$ ) of a neutron star and provides a unique bridge between atomic nuclei and neutron star [25]. The large value of  $\Delta r_{np} = 0.283 \pm 0.071$  fm suggests a large value of  $L$  which yields a very stiff EOS. This generally gives rise to a large value of neutron star radius and the tidal deformability [3]. The upper limit on  $\Lambda_{1.4} \leq 580$  for GW170817 requires softer EOS and hence softer symmetry energy coefficient [18]. The heaviest observed neutron star  $M_{max} = 2.35 \pm 0.17 M_{\odot}$  for the black-widow pulsar PSR J0952-0607 [26] may place stringent constraints on the symmetry energy at high densities, since, the EOS of symmetric nuclear matter (SNM) from heavy ion collisions flow data [27] which is relatively soft and limits the NS maximum mass.

\* virenthakur2154@gmail.com

† raj.phy@gmail.com

‡ sinp.bijay@gmail.com

§ shashi.dhiman@gmail.com

The motivation of the present work is to generate a new parametrization of the RMF model which can accommodate the properties of NSs within the astrophysical observations without compromising the finite nuclei properties. The RMF model used in the present work, includes all possible self and mixed-coupling terms for the  $\sigma$ ,  $\omega$ , and  $\rho$  mesons up to the quartic order so that the parameters should obey the naturalness behavior as imposed by the effective field theory [28]. In this work, the new parameter set is searched in view of PREX-II data and the model EOS satisfies the observed astrophysical constraints imposed by NSs.

The paper is organized as follows, in section II, the theoretical framework which is used to construct the EOS for neutron stars has been discussed. In section III, the procedure for optimization and covariance analysis of the parameters is discussed. In section IV, we present our results. Finally, we summarized the results of the present work in section V.

## II. THEORETICAL MODEL

The effective lagrangian density for the RMF model generally describes the interaction of the baryons via the exchange of  $\sigma$ ,  $\omega$ , and  $\rho$  mesons up to the quartic order. The Lagrangian density[5, 7, 29] is given by

$$\begin{aligned}
\mathcal{L} = & \sum_B \bar{\Psi}_B [i\gamma^\mu \partial_\mu - (M_B - g_{\sigma B}\sigma) - (g_{\omega B}\gamma^\mu \omega_\mu \\
& + \frac{1}{2}g_{\rho B}\gamma^\mu \tau_B \cdot \rho_\mu)] \Psi_B + \frac{1}{2}(\partial_\mu \sigma \partial^\mu \sigma - m_\sigma^2 \sigma^2) \\
& - \frac{\bar{\kappa}}{3!}g_{\sigma N}^3 \sigma^3 - \frac{\bar{\lambda}}{4!}g_{\sigma N}^4 \sigma^4 - \frac{1}{4}\omega_{\mu\nu}\omega^{\mu\nu} + \frac{1}{2}m_\omega^2 \omega_\mu \omega^\mu \\
& + \frac{1}{4!}\zeta g_{\omega N}^4 (\omega_\mu \omega^\mu)^2 - \frac{1}{4}\rho_{\mu\nu}\rho^{\mu\nu} + \frac{1}{2}m_\rho^2 \rho_\mu \rho^\mu \\
& + \frac{1}{4!}\xi g_{\rho N}^4 (\rho_\mu \rho^\mu)^2 \\
& + g_{\sigma N}g_{\omega N}^2 \sigma \omega_\mu \omega^\mu \left( a_1 + \frac{1}{2}a_2 \sigma \right) \\
& + g_{\sigma N}g_{\rho N}^2 \sigma \rho_\mu \rho^\mu \left( b_1 + \frac{1}{2}b_2 \sigma \right) \\
& + \frac{1}{2}c_1 g_{\omega N}^2 g_{\rho N}^2 \omega_\mu \omega^\mu \rho_\mu \rho^\mu
\end{aligned} \quad (1)$$

The equation of motion for baryons, mesons, and photons can be derived from the Lagrangian density defined in Eq.(1). The equation of motion for baryons can be given as,

$$\begin{aligned}
\left[ \gamma^\mu \left( i\partial_\mu - g_{\omega B}\omega_\mu - \frac{1}{2}g_{\rho B}\tau_B \cdot \rho_\mu - e\frac{1+\tau_3 B}{2}A_\mu \right) - \right. \\
\left. (M_B + g_{\sigma B}\sigma) \right] \Psi_B = \epsilon_B \Psi_B.
\end{aligned} \quad (2)$$

The Euler-Lagrange equations for the ground-state expectation values of the mesons fields are

$$\begin{aligned}
(-\Delta + m_\sigma^2)\sigma = & \sum_B g_{\sigma B}\rho_{sB} - \frac{\bar{\kappa}}{2}g_{\sigma N}^3 \sigma^2 - \frac{\bar{\lambda}}{6}g_{\sigma N}^4 \sigma^3 \\
& + a_1 g_{\sigma N}g_{\omega N}^2 \omega^2 + a_2 g_{\sigma N}^2 g_{\omega N}^2 \sigma \omega^2 \\
& + b_1 g_{\sigma N}g_{\rho N}^2 \rho^2 + b_2 g_{\sigma N}^2 g_{\rho N}^2 \sigma \rho^2,
\end{aligned} \quad (3)$$

$$\begin{aligned}
(-\Delta + m_\omega^2)\omega = & \sum_B g_{\omega B}\rho_B - \frac{\zeta}{6}g_{\omega N}^4 \omega^3 \\
& - 2a_1 g_{\sigma N}g_{\omega N}^2 \sigma \omega - a_2 g_{\sigma N}^2 g_{\omega N}^2 \sigma^2 \omega \\
& - c_1 g_{\omega N}^2 g_{\rho N}^2 \omega \rho^2,
\end{aligned} \quad (4)$$

$$\begin{aligned}
(-\Delta + m_\rho^2)\rho = & \sum_B g_{\rho B}\tau_{3B}\rho_B - \frac{\xi}{6}g_{\rho N}^4 \rho^3 \\
& - 2b_1 g_{\sigma N}g_{\rho N}^2 \sigma \rho - b_2 g_{\sigma N}^2 g_{\rho N}^2 \sigma^2 \rho \\
& - c_1 g_{\omega N}^2 g_{\rho N}^2 \omega^2 \rho,
\end{aligned} \quad (5)$$

$$-\Delta A_0 = e\rho_p. \quad (6)$$

where the baryon vector density  $\rho_B$ , scalar density  $\rho_{sB}$  and charge density  $\rho_p$  are, respectively,

$$\rho_B = \langle \bar{\Psi}_B \gamma^0 \Psi_B \rangle = \frac{\gamma k_B^3}{6\pi^2}, \quad (7)$$

$$\rho_{sB} = \langle \bar{\Psi}_B \Psi_B \rangle = \frac{\gamma}{(2\pi)^3} \int_0^{k_B} d^3k \frac{M_B^*}{\sqrt{k^2 + M_B^*}}, \quad (8)$$

$$\rho_p = \left\langle \bar{\Psi}_B \gamma^0 \frac{1 + \tau_{3B}}{2} \Psi_B \right\rangle, \quad (9)$$

with  $\gamma$  the spin-isospin degeneracy. The  $M_B^* = M_B - g_{\sigma B}\sigma$  is the effective mass of the baryon species B,  $k_B$  is its Fermi momentum and  $\tau_{3B}$  denotes the isospin projections of baryon B. The energy density of the uniform matter within the framework of the RMF model is given by;

$$\begin{aligned}
\mathcal{E} = & \sum_{j=B,\ell} \frac{1}{\pi^2} \int_0^{k_j} k^2 \sqrt{k^2 + M_j^{*2}} dk \\
& + \sum_B g_{\omega B}\omega \rho_B + \sum_B g_{\rho B}\tau_{3B}\rho_B + \frac{1}{2}m_\sigma^2 \sigma^2 \\
& + \frac{\bar{\kappa}}{6}g_{\sigma N}^3 \sigma^3 + \frac{\bar{\lambda}}{24}g_{\sigma N}^4 \sigma^4 - \frac{\zeta}{24}g_{\omega N}^4 \omega^4 \\
& - \frac{\xi}{24}g_{\rho N}^4 \rho^4 - \frac{1}{2}m_\omega^2 \omega^2 - \frac{1}{2}m_\rho^2 \rho^2 \\
& - a_1 g_{\sigma N}g_{\omega N}^2 \sigma \omega^2 - \frac{1}{2}a_2 g_{\sigma N}^2 g_{\omega N}^2 \sigma^2 \omega^2 \\
& - b_1 g_{\sigma N}g_{\rho N}^2 \sigma \rho^2 - \frac{1}{2}b_2 g_{\sigma N}^2 g_{\rho N}^2 \sigma^2 \rho^2 \\
& - \frac{1}{2}c_1 g_{\omega N}^2 g_{\rho N}^2 \omega^2 \rho^2.
\end{aligned} \quad (10)$$

The pressure of the uniform matter is given by

$$\begin{aligned}
P = & \sum_{j=B,\ell} \frac{1}{3\pi^2} \int_0^{k_j} \frac{k^4 dk}{\sqrt{k^2 + M_j^{*2}}} - \frac{1}{2} m_\sigma^2 \sigma^2 \\
& - \frac{\bar{\kappa}}{6} g_{\sigma N}^3 \sigma^3 - \frac{\bar{\lambda}}{24} g_{\sigma N}^4 \sigma^4 + \frac{\zeta}{24} g_{\omega N}^4 \omega^4 \\
& + \frac{\xi}{24} g_{\rho N}^4 \rho^4 + \frac{1}{2} m_\omega^2 \omega^2 + \frac{1}{2} m_\rho^2 \rho^2 \\
& + a_1 g_{\sigma N} g_{\omega N}^2 \sigma \omega^2 + \frac{1}{2} a_2 g_{\sigma N}^2 g_{\omega N}^2 \sigma^2 \omega^2 \\
& + b_1 g_{\sigma N} g_{\rho N}^2 \sigma \rho^2 + \frac{1}{2} b_2 g_{\sigma N}^2 g_{\rho N}^2 \sigma^2 \rho^2 \\
& + \frac{1}{2} c_1 g_{\omega N}^2 g_{\rho N}^2 \omega^2 \rho^2.
\end{aligned} \tag{11}$$

Here, the sum is taken over nucleons and leptons.

### III. OPTIMIZATION AND COVARIANCE ANALYSIS

The optimization of the parameters ( $\mathbf{p}$ ) appearing in the Lagrangian (Eq. 1) has been performed by using the simulated annealing method (SAM) [30, 31] by following  $\chi^2$  minimization procedure which is given as,

$$\chi^2(\mathbf{p}) = \frac{1}{N_d - N_p} \sum_{i=1}^{N_d} \left( \frac{M_i^{exp} - M_i^{th}}{\sigma_i} \right)^2, \tag{12}$$

where  $N_d$  is the number of experimental data points and  $N_p$  is the number of fitted parameters. The  $\sigma_i$  denotes adopted errors [32] and  $M_i^{exp}$  and  $M_i^{th}$  are the experimental and the corresponding theoretical values, respectively, for a given observable. The minimum value of  $\chi_0^2$  corresponds to the optimal values  $\mathbf{p}_0$  of the parameters. Following the optimization of the energy density functional, it is important to explore the richness of the covariance analysis. It enables one to calculate the statistical uncertainties on model parameters or any calculated physical observables. The covariance analysis also provides additional information about the sensitivity of the parameters to the physical observables, and interdependence among the parameters [32–35]. Having obtained the parameter set, the correlation coefficient between two quantities Y and Z can be calculated by covariance analysis [32, 34–37] as

$$c_{YZ} = \frac{\overline{\Delta Y \Delta Z}}{\sqrt{\overline{\Delta Y^2} \overline{\Delta Z^2}}}, \tag{13}$$

where covariance between Y and Z is expressed as

$$\overline{\Delta Y \Delta Z} = \sum_{\alpha\beta} \left( \frac{\partial Y}{\partial p_\alpha} \right)_{\mathbf{p}_0} C_{\alpha\beta}^{-1} \left( \frac{\partial Z}{\partial p_\beta} \right)_{\mathbf{p}_0}. \tag{14}$$

Here,  $C_{\alpha\beta}^{-1}$  is an element of inverted curvature matrix given by

$$C_{\alpha\beta} = \frac{1}{2} \left( \frac{\partial^2 \chi^2(\mathbf{p})}{\partial p_\alpha \partial p_\beta} \right)_{\mathbf{p}_0}. \tag{15}$$

The standard deviation,  $\overline{\Delta Y^2}$ , in Y can be computed using Eq. (14) by substituting  $Z = Y$ . The prediction of maximum mass around  $2M_\odot$  for the nonrotating neutron star and constraints on EOSs of Symmetric Nuclear Matter (SNM) and Pure Neutron Matter (PNM) as extracted from the analysis of particle flow in heavy ion collisions [27] require relatively softer EOSs as demanded by GW170817 event.

### IV. RESULTS AND DISCUSSION

The parameters of the model are searched by fit to the available experimental data of total binding energies and charge rms radii [38–40] for some closed/open shell nuclei  $^{16,24}\text{O}$ ,  $^{40,48,54}\text{Ca}$ ,  $^{56,68,78}\text{Ni}$ ,  $^{88}\text{Sr}$ ,  $^{90}\text{Zr}$ ,  $^{100,116,132,138}\text{Sn}$ , and  $^{144}\text{Sm}$ ,  $^{208}\text{Pb}$ . We have also included the maximum mass of neutron star [41] in our fit data. Recently, the parity-violating electron scattering experiment (PREX-II) put a limit on the neutron skin thickness of  $^{208}\text{Pb}$  is  $\Delta r_{np} = 0.283 \pm 0.071$  fm [24]. We included the recently measured  $\Delta r_{np}$  in our fit data to constrain the linear density dependence of symmetry energy coefficient. For the open shell nuclei, the pairing has been included by using BCS formalism with constant pairing gaps that have been taken from the particle separation energies of neighboring nuclei [42–44]. In Table I, we display the values of relativistic parameterization DBHP generated for the Lagrangian given by Eq. (1) along with theoretical uncertainties. The values of parameter sets for NL3 [45], FSUGarnet [33], IOPB-1 [46] and Big Apple [47] are also shown.

The effective field theory imposes the condition of naturalness [28] on the parameters or expansion coefficients appearing in the effective Lagrangian density Eq. (1). According to naturalness, the coefficients of various terms in Lagrangian density functional should be of the same size when expressed in an appropriate dimensionless ratio. The dimensionless ratios are obtained by dividing Eq. (1) by  $M^4$  and expressing each term in powers of  $\frac{g_\sigma \sigma}{M}$ ,  $\frac{g_\omega \omega}{M}$  and  $2\frac{g_\rho \rho}{M}$ . This means that the dimensionless ratios  $\frac{1}{2C_\sigma^2 M^2}$ ,  $\frac{1}{2C_\omega^2 M^2}$ ,  $\frac{1}{8C_\rho^2 M^2}$ ,  $\frac{\bar{\kappa}}{6M}$ ,  $\frac{\bar{\lambda}}{24}$ ,  $\frac{\zeta}{24}$ ,  $\frac{a_1}{M}$ ,  $\frac{a_2}{2}$ ,  $\frac{b_1}{4M}$ ,  $\frac{b_2}{8}$  and  $\frac{c_1}{8}$  should be roughly of same size, where  $c_i^2 = \frac{g_i^2}{M_i^2}$ , i denotes  $\sigma$ ,  $\omega$  and  $\rho$  mesons. In Table II, we present the overall naturalness behavior of DBHP parameterization i.e. the value of these parameters when expressed in dimensionless ratios as shown just above. We also display the corresponding values for NL3, FSUGarnet, IOPB-1, and Big Apple parameter sets. It is obvious from the table that DBHP parameterization closely favors the naturalness behavior. This may be attributed to the fact that this parameterization includes all possible self and crossed interaction terms of  $\sigma$ ,  $\omega$ , and  $\rho$ -mesons up to the quartic order.

The small value of parameter  $c_1$  for DBHP model which gives rise to better naturalness behaviour of the parameters might be attributed to the fact that the coupling

TABLE I. New parameter set for DBHP model of RMF Lagrangian given in Eq.(1) along with theoretical uncertainties. The parameters  $\bar{\kappa}$ ,  $a_1$ , and  $b_1$  are in  $\text{fm}^{-1}$ . The masses  $m_\sigma, m_\omega$  and  $m_\rho$  values are in MeV. The mass for nucleon is taken as  $M_N = 939\text{MeV}$ . The values of  $\bar{\kappa}$ ,  $\bar{\lambda}$ ,  $a_1$ ,  $a_2$ ,  $b_1$ ,  $b_2$ , and  $c_1$  are multiplied by  $10^2$ . Parameters for NL3, FSUGarnet, IOPB-1, and Big Apple are also shown for comparison.

Parameters	DBHP	NL3	FSUGarnet	IOPB-1	Big Apple
$g_\sigma$	10.34155±0.06660	10.21743	10.50315	10.41851	9.67810
$g_\omega$	13.30826±0.10044	12.86762	13.69695	13.38412	12.33541
$g_\rho$	11.25845±1.31969	8.94800	13.87880	11.11560	14.14256
$\bar{\kappa}$	1.82166±0.05101	1.95734	1.65229	1.85581	2.61776
$\bar{\lambda}$	0.24446±0.17154	-1.59137	-0.03533	-0.07552	-2.16586
$\zeta$	0.02156±0.00401	0.00000	0.23486	0.01744	0.00070
$a_1$	0.01172±0.00383	0.00000	0.00000	0.00000	0.00000
$a_2$	0.05281 ±0.03677	0.00000	0.00000	0.00000	0.00000
$b_1$	0.39811±0.40926	0.00000	0.00000	0.00000	0.00000
$b_2$	0.09412±1.85465	0.00000	0.00000	0.00000	0.00000
$c_1$	0.79914±3.15145	0.00000	8.60000	4.80000	9.40000
$m_\sigma$	501.04834±1.34831	508.19400	496.73100	500.48700	492.97500
$m_\omega$	782.50000	782.50100	782.18700	782.18700	782.18700
$m_\rho$	770.00000	763.00000	762.46800	762.46800	762.46800

parameter  $c_1$  has strong correlation with  $b_1$  and also has good correlation with  $a_2$  and  $b_2$  (see Fig. 1). It is evident from the table that the value of coupling parameter  $c_1$  (crossed interaction term of  $\omega^2$  and  $\rho^2$ ) appearing in Eq. (1) is large for IOPB-I, FSU-Garnet and Big Apple which shows deviation from the naturalness behavior in the absence of all other possible mixed interaction terms of  $\sigma$ ,  $\omega$ , and  $\rho$ -meson. Keeping in view the naturalness behavior of the parameters as imposed by the effective field theory [28] and as observed in case of DBHP model, it is important to incorporate the contributions of the higher order mixed interactions of mesons in the Lagrangian. The naturalness behavior of parameters can be further improved by considering the next higher order terms containing the gradient of fields [28]. As far as NL3 parameterization is concerned, the naturalness behavior is favored very well but it does not include any cross interaction terms of  $\sigma$ ,  $\omega$ , and  $\rho$  mesons which are very important for constraining the symmetry energy and its density dependence.

In Fig.1, the correlation coefficients between the DBHP model parameter appearing in Lagrangian (Eq. 1) are shown in graphical form. A strong correlation is found between the pairs of model parameters  $g_\sigma$  and  $g_\omega$  (0.95),  $c_1 - b_1$  (0.80), and  $a_2 - \bar{\kappa}$  (0.72). The strong correlation is also found for  $g_\rho$  with  $b_1$  and  $b_2$ . Mild correlations exist between the pairs of model parameters  $g_\sigma - \bar{\kappa}$ ,  $g_\sigma - a_1$  and  $g_\sigma - a_2$ . A strong correlation between the model parameters implies a strong interdependence i.e. if one parameter is fixed at a certain value then the other must attain the precise value as suggested by their correlation.

## A. Properties of finite nuclei and nuclear matter

The newly generated DBHP parameterization gives a good fit to the properties of finite nuclei. In Fig. 2, we display the value of relative error in the total binding energies  $\delta E = \frac{B^{exp} - B^{th}}{B^{exp}}$  calculated for DBHP parameterization. We also display similar results for other parameter sets considered. It is evident that binding energies obtained using DBHP parameterization are in good agreement with the available experimental data [48]. The root mean square (rms) errors in total binding energy for all the nuclei considered in our fit data is found to be 2.1 MeV. In Fig.3, we present our results for relative error  $\delta R_{ch}$  for charge rms radii and also compare them with other parameter sets. The root mean square (rms) errors in charge radii for all nuclei taken in our fit is 0.02 fm. The neutron skin thickness of  $^{208}\text{Pb}$  for DBHP model comes out to be  $0.24 \pm 0.02$  fm. In Table III, we present the results for the SNM properties such as binding energy per nucleon (E/A), incompressibility (K), the effective nucleon mass ( $M^*$ ) at the saturation density ( $\rho_0$ ), symmetry energy coefficient (J), slope of symmetry energy (L) and curvature parameter  $K_{\text{sym}}$  along with the theoretical uncertainties. It is observed that the isoscalar properties (E/A, K,  $M^*$ ,  $\rho_0$ ) are well constrained for DBHP parameterization (at the  $\leq 3.3$  % level). But in isovector sector, the error on the density dependence of the symmetry energy are relatively larger for  $L$  ( $\approx 23$  %). The value of  $K_{\text{sym}}$  is determined only poorly [49–51]. The experimental data on finite nuclei are not enough to constrain  $K_{\text{sym}}$ . Only the accurate knowledge of symmetry energy at higher densities ( $\rho > 2\rho_0$ ) may constrain the  $K_{\text{sym}}$  in tighter bounds. This may be attributed to the large experimental error on the neutron skin thickness for  $^{208}\text{Pb}$  ( $0.283 \pm 0.071$  fm) which

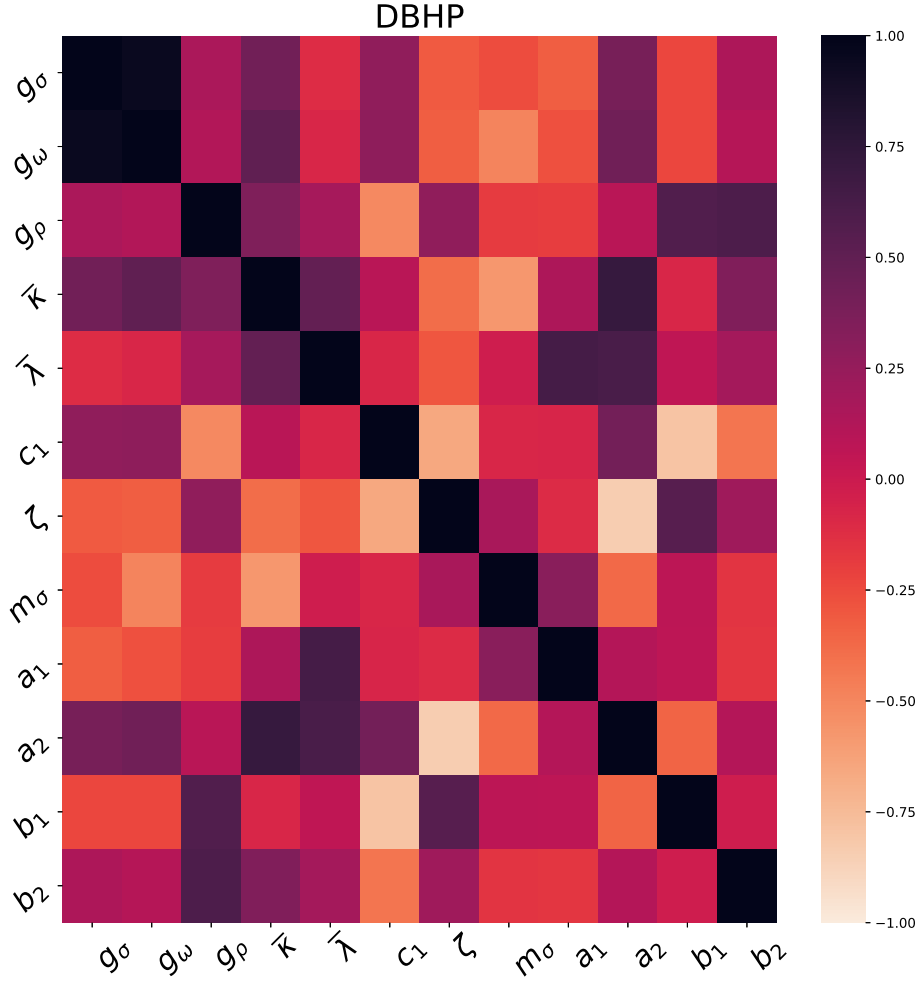


FIG. 1. (Color online) Correlation coefficients among the model parameters for DBHP parametrization of the Lagrangian given by Eq. (1).

TABLE II. The values of parameters are expressed as dimensionless ratios corresponding to naturalness behavior. All values have been multiplied by  $10^3$ .

Parameters	DBHP	NL3	FSUGarnet	IOPB-1	Big Apple
$\frac{1}{2C^2 M^2}$	1.3311	1.4028	1.2690	1.3086	1.4698
$\frac{1}{2C^2 M^2}$	1.9604	2.0970	1.8508	1.9383	2.2819
$\frac{1}{8C^2 M^2}$	0.6631	1.0306	0.4278	0.6670	0.4121
$\frac{\kappa}{6M}$	0.6380	0.6855	0.5787	0.6499	0.9168
$\frac{\lambda}{24}$	0.1018	-0.6630	-0.1472	-0.3146	-0.9024
$\frac{\zeta}{24}$	0.8982	-	0.9785	0.7267	0.0291
$\frac{a_1}{M}$	0.1172	-	-	-	-
$\frac{a_2}{2}$	0.2641	-	-	-	-
$\frac{b_1}{4M}$	0.9953	-	-	-	-
$\frac{b_2}{8}$	0.1177	-	-	-	-
$\frac{c_1}{8}$	0.9989	-	10.7500	6.0000	11.7500

TABLE III. The bulk nuclear matter properties (NMPs) at saturation density along with calculated theoretical errors for DBHP parameterization compared with that other parameter sets.  $\rho_0$ ,  $E/A$ ,  $K$ ,  $M^*/M$ ,  $J$ ,  $L$  and  $K_{sym}$  denote the saturation density, Binding Energy per nucleon, Nuclear Matter incompressibility coefficient, the ratio of effective nucleon mass to the nucleon mass, Symmetry Energy, the slope of symmetry energy, and curvature of symmetry energy respectively. the value of  $\rho_0$  is in  $\text{fm}^{-3}$  and rest all the quantities are in MeV. The values of neutron skin thickness  $\Delta r_{np}$  for  $^{208}\text{Pb}$  and  $^{48}\text{Ca}$  nuclei in units of fm are also listed.

$NMPs$	DBHP	NL3	FSUGarnet	IOPB-1	Big Apple
$\rho_0$	$0.148 \pm 0.003$	0.148	0.153	0.149	0.155
$E/A$	$-16.11 \pm 0.05$	-16.25	-16.23	-16.09	-16.34
$K$	$229.5 \pm 5.6$	271.6	229.6	222.6	227.1
$M^*/M$	$0.615 \pm 0.007$	0.595	0.578	0.595	0.608
$J$	$34.7 \pm 1.5$	37.4	30.9	33.3	31.4
$L$	$83.9 \pm 19.2$	118.6	50.9	63.8	40.3
$K_{sym}$	$-33.2 \pm 64.1$	100.7	57.9	-38.4	88.8
$\Delta r_{np}$ ( $^{208}\text{Pb}$ )	$0.24 \pm 0.02$	0.28	0.16	0.22	0.15
$\Delta r_{np}$ ( $^{48}\text{Ca}$ )	$0.21 \pm 0.02$	0.23	0.17	0.17	0.17

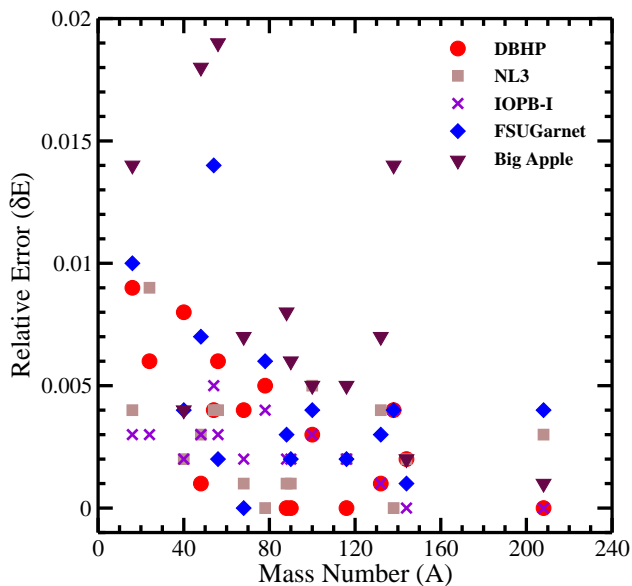


FIG. 2. (Color online) Relative error in the total binding energy ( $\delta E$ ) plotted against the mass number ( $A$ ) for the newly generated parameter set DBHP. For comparison, the values of  $\delta E$  obtained with parameters NL3, IOPB-1, FSUGarnet and Big Apple are also displayed.

lead us choosing the large adopted error during the optimisation procedure. The values of neutron-skin thickness ( $\Delta r_{np}$ ) for  $^{208}\text{Pb}$  and  $^{48}\text{Ca}$  nuclei are also presented. The DBHP parameter significantly overestimates the value of neutron-skin thickness for  $^{48}\text{Ca}$  in comparison to that  $\Delta r_{np}(^{48}\text{Ca}) = 0.121 \pm 0.026$  fm as reported recently by CREX [52]. Other parametrizations considered in Table III also do not satisfy simultaneously the experimental data for the neutron-skin for the  $^{208}\text{Pb}$  and  $^{48}\text{Ca}$  nuclei. Similar trends have been observed in recent investigations based on the relativistic and non-relativistic mean

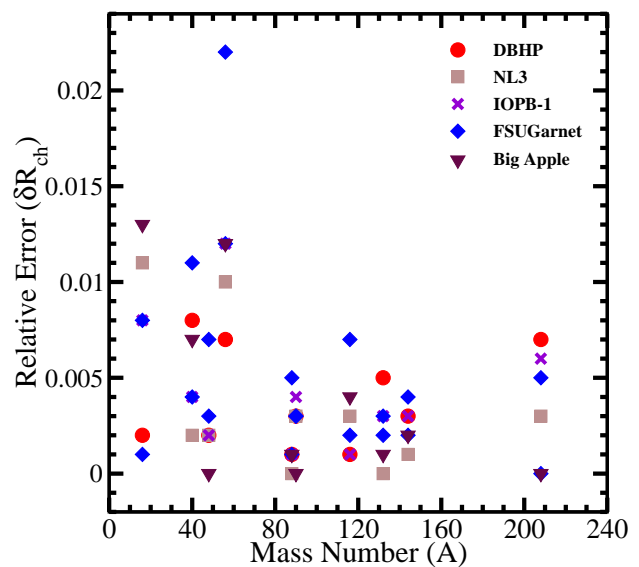


FIG. 3. (Color online) Relative error in the charge root mean square ( $\delta R_{ch}$ ) plotted against the mass number ( $A$ ) for the newly generated parameter set DBHP. For comparison, the values obtained with parameters NL3, IOPB-1, FSUGarnet and Big Apple are also displayed.

field models which call for further experimental studies [53–55].

The results are also compared with the NL3 [45], FSUGarnet [33], IOPB-1 [46] and Big Apple [47] parameter sets. These SNM properties are very important for constructing the EOS for nuclear matter.  $E/A$  is  $-16.1$  MeV for DBHP parameterization. The value of  $J$  and  $L$  obtained by DBHP parameterization are consistent with the values  $J = 38.1 \pm 4.7$  MeV and  $L = 106 \pm 37$  MeV as inferred by Reed et. al., [3]. The value of  $K$  is  $225$  MeV which is in agreement with the value  $K = 240 \pm 20$  MeV determined from isoscalar giant monopole reso-

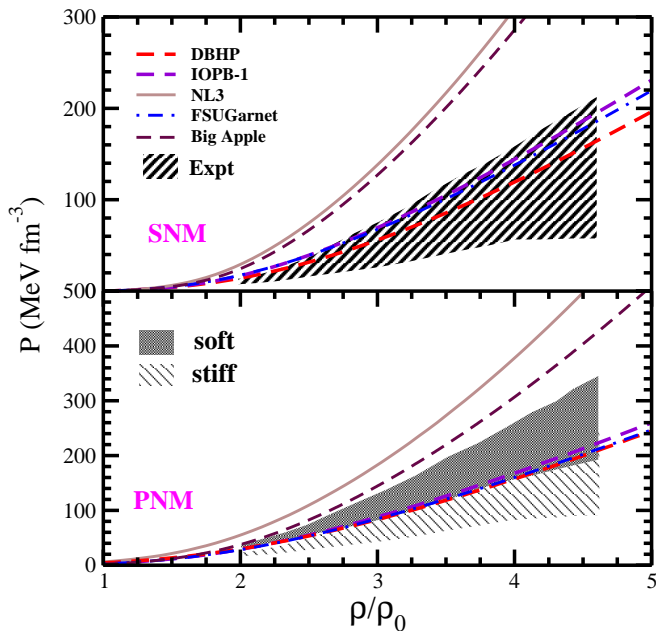


FIG. 4. (color online) Variation of Pressure as a function of baryon density for SNM (upper panel) and PNM (lower panel) computed with DBHP parameterization along with NL3, IOPB-1, FSUGarnet and Big Apple models. The shaded region represents the experimental data taken from the reference [27].

nance (ISGMR) for  $^{90}\text{Zr}$  and  $^{208}\text{Pb}$  nuclei [56, 57].

In Fig. 4, we plot the EOS i.e. pressure as a function of the baryon density for SNM (upper) and PNM (lower panel) using the DBHP parameterization that agrees reasonably well and lies in the allowed region with the EOS extracted from the analysis of the particle flow in heavy ion collision [27]. It is evident from the figure that the EOSs for SNM and PNM calculated with the NL3 parameterization are very stiff and ruled out by the heavy ion collision data. The EOS calculated by using the DBHP parameterization is relatively softer which is in requirement to constrain the recent astrophysical observations [41, 58–60]. In Fig. 5, we plot the symmetry energy as a function of baryon density for DBHP model. The results for other parametrizations are also shown for comparison. It can be observed that the symmetry energy increases with baryon density and it is found to be softer than NL3 but stiffer than IOPB-1, FSUGarnet and Big Apple models.

## B. Neutron star properties

In Fig. 6 we display the variation of pressure with the energy density for the nucleonic matter in  $\beta$  equilibrium for the DBHP parameterization. The results are also compared with those obtained for parameter sets. The shaded region represents the observational constraints at  $r_{ph} = R$  with the  $2\sigma$  uncertainty [58]. Here  $r_{ph}$  and  $R$  are

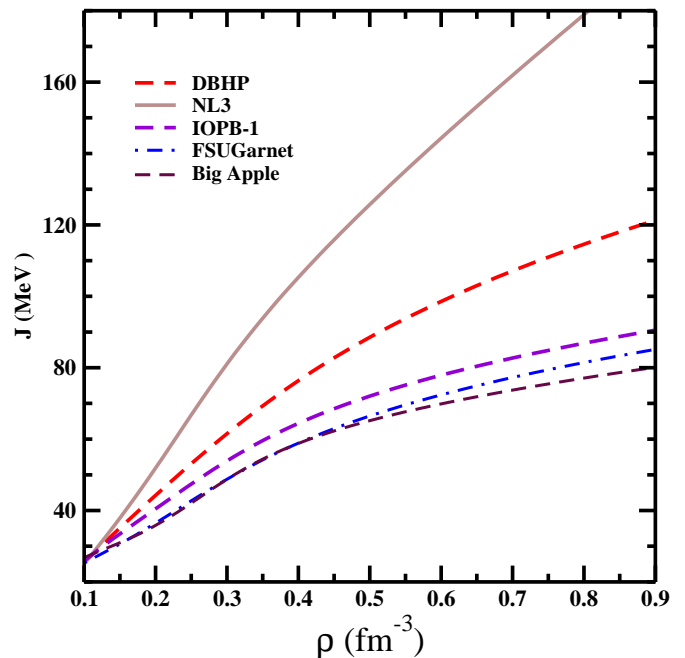


FIG. 5. (Color online) The density dependent symmetry energy plotted as a function of baryon density for DBHP model. The results are also displayed for NL3, IOPB-1, FSUGarnet and Big Apple parameter sets.

the photospheric and neutron star radius respectively. It is clear that the EOS computed with our DBHP parameter set is consistent with the EOS obtained by Steiner et al. [58].

The EOSs obtained by the DBHP and IOPB-1 parameterizations are softer and lie in the allowed shaded region which represents the observational constraints taken from Ref. [58]. The EOS obtained with NL3 parameter set is much stiffer than DBHP and IOPB-1 parameter sets and ruled out by the observational constraints [58]. The stiffness of EOS for NL3 may be attributed to its very high value of compressibility ( $K$ ), symmetry energy coefficient ( $J$ ), and slope of symmetry energy ( $L$ ) as shown in Table (III). The mass and radius of a neutron star are obtained by solving the Tolman-Oppenheimer-Volkoff (TOV) equations [61, 62] given as:

$$\frac{dP(r)}{dr} = -\frac{\{\epsilon(r) + P(r)\}\{4\pi r^3 P(r) + m(r)\}}{r^2(1 - 2m(r)/r)} \quad (16)$$

$$\frac{dm}{dr} = 4\pi r^2 \epsilon(r), \quad (17)$$

$$m(r) = 4\pi \int_0^r dr r^2 \epsilon(r) \quad (18)$$

where  $P(r)$  is the pressure at radial distance  $r$  and  $m(r)$  is the mass of neutron stars enclosed in the sphere of radius  $r$ . The EOS for the crust region is taken from Ref.

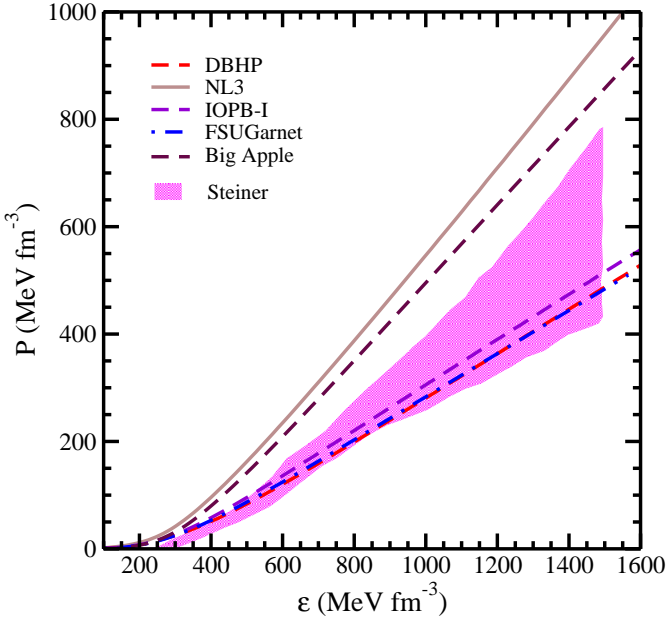


FIG. 6. (color online) Variation of Pressure as a function of Energy Density for DBHP parameter set. EOS computed with NL3, IOPB-1, FSUGarnet and Big Apple models are also shown for comparison. The Shades region represents the observational constraints taken from reference [58].

[63]. In Fig. 7 we present our results for gravitational mass of static neutron star and its radius for DBHP and other parameterizations.

It is observed that the maximum gravitational mass of the static neutron star for DBHP parameter set is  $2.03 M_{\odot}$  which is in good agreement with the mass constraints from GW170817 event, pulsars PSRJ1614-2230, PSRJ0348+0432, and PSRJ0740+6620 [16, 41, 59, 60, 64]. The radius ( $R_{1.4}$ ) of canonical mass is 13.39 Km for DBHP parameterization which satisfies the radius constraints from NICER [59, 60, 65]. The value of  $R_{1.4}$  for NL3 parameterization is 14.61 Km which seems to rule out the constraints for  $R_{1.4}$  extracted from Ref. [66].

The tidal deformability  $\Lambda$  rendered by the companion stars on each other in a binary system can provide remarkable pieces of information on the EOS of neutron stars [67, 68]. The tidal influences of its companion in BNS system will deform neutron stars in the binary system and, the resulting change in the gravitational potential modifies the BNS orbital motion and its corresponding gravitational wave (GW) signal. This effect on GW phasing can be parameterized by the dimensionless tidal deformability parameter,  $\Lambda_i = \lambda_i/M_i^5$ ,  $i = 1, 2$ . For each neutron star, its quadrupole moment  $Q_{j,k}$  must be related to the tidal field  $\mathcal{E}_{j,k}$  caused by its companion as,  $Q_{j,k} = -\lambda\mathcal{E}_{j,k}$ , where,  $j$  and  $k$  are spatial tensor indices. The dimensionless tidal deformability parameter  $\Lambda$  of a static, spherically symmetric compact star depends on the neutron star compactness parameter  $C$  and a dimensionless quadrupole Love number  $k_2$  as,  $\Lambda = \frac{2}{3}k_2C^{-5}$ .

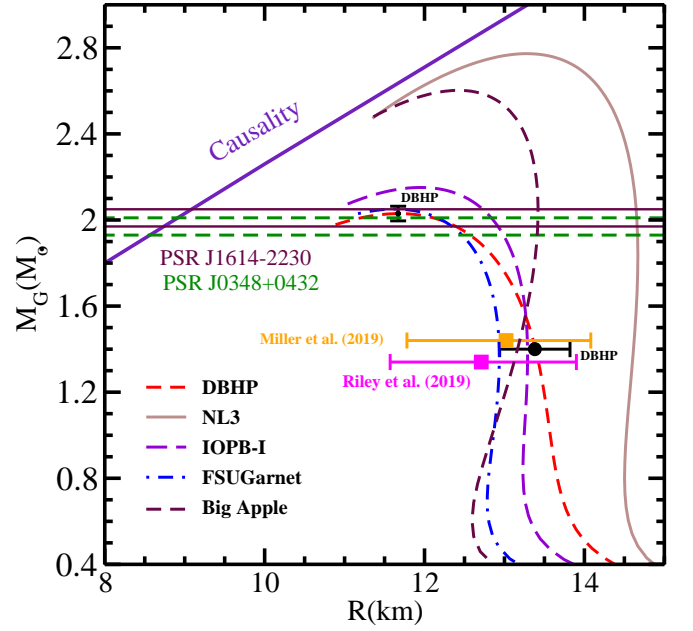


FIG. 7. (color online) Relationship between neutron star mass and its radius for DBHP parameterization. The results are compared with NL3, IOPB-1, FSUGarnet and Big Apple parameters.

The  $\Lambda$  critically parameterizes the deformation of neutron stars under the given tidal field, therefore it should depend on the EOS of nuclear dense matter. To measure the Love number  $k_2$  along with the evaluation of the TOV equations we have to compute  $y_2 = y(R)$  with initial boundary condition  $y(0) = 2$  from the first-order differential equation [67–70] simultaneously,

$$y' = \frac{1}{r}[-r^2Q - ye^\lambda\{1 + 4\pi Gr^2(P - \mathcal{E})\} - y^2], \quad (19)$$

$$Q \equiv 4\pi Ge^\lambda(5\mathcal{E} + 9P + \frac{\mathcal{E} + P}{c_s^2}) - 6\frac{e^\lambda}{r^2} - \nu'^2 \quad (20)$$

$$e^\lambda \equiv (1 - \frac{2Gm}{r})^{-1} \quad (21)$$

$$\nu' \equiv 2Ge^\lambda(\frac{m + 4\pi Pr^3}{r^2}). \quad (22)$$

First, we get the solutions of Eq.(19) with boundary condition,  $y_2 = y(R)$ , then the electric tidal Love number  $k_2$  is calculated from the expression as,

$$k_2 = \frac{8}{5}C^5(1 - 2C)^2[2C(y_2 - 1) - y_2 + 2]\{2C(4(y_2 + 1)C^4 + (6y_2 - 4)C^3 + (26 - 22y_2)C^2 + 3(5y_2 - 8)C - 3y_2 + 6) - 3(1 - 2C)^2(2C(y_2 - 1) - y_2 + 2)\log(\frac{1}{1 - 2C})\}^{-1}. \quad (23)$$

Fig. 8 shows the results of dimensionless tidal deformability  $\Lambda$  as a function of gravitational mass for neutron stars for DBHP and other parameterizations. The value of  $\Lambda$  decreases with an increase in the gravitational mass



TABLE IV. The properties of nonrotating neutron stars along with theoretical uncertainties obtained for the DBHP parameter set. Results are also compared with the other parameter sets.  $M_{max}$  and  $R_{max}$  denote the Maximum Gravitational mass and corresponding radius, respectively. The values for  $R_{1.4}$  and  $\Lambda_{1.4}$  denote radius and dimensionless tidal deformability at  $1.4M_{\odot}$ .

EOS	M ( $M_{\odot}$ )	$R_{max}$ (km)	$R_{1.4}$ (km)	$\Lambda_{1.4}$
DBHP	$2.03 \pm 0.04$	$11.68 \pm 0.29$	$13.39 \pm 0.41$	$682 \pm 125$
NL3	2.77	13.27	14.61	1254
IOPB-I	2.15	11.95	13.28	694
FSUGarnet	2.06	11.70	12.86	624
Big Apple	2.6	12.41	12.96	717

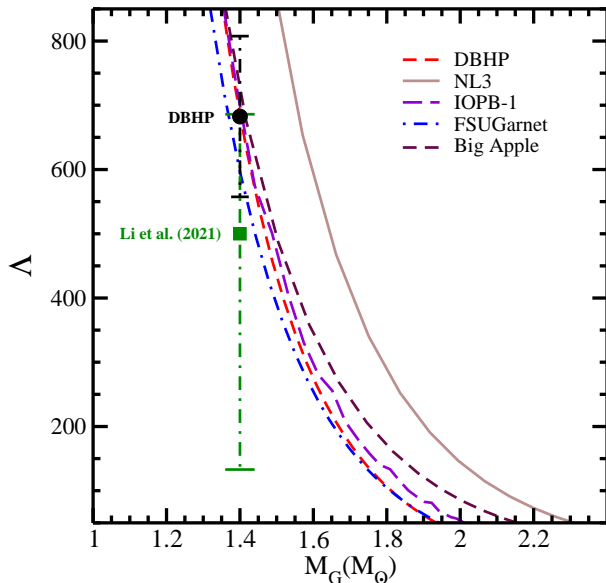


FIG. 8. (Color online) Variation of dimensionless tidal deformability ( $\Lambda$ ) with respect to gravitational mass for DBHP parameterization. The results for NL3, IOPB-1, FSUGarnet and Big Apple parameters are also shown.

of the neutron star and reduces to a very small value at the maximum mass. The value of  $\Lambda_{1.4}$  obtained for canonical mass with DBHP parameters is  $682 \pm 125$  which satisfies the finding from the GW170817 event [3, 71, 72] for the EOS of dense nuclear matter.

It is noteworthy that the our analysis of tidal deformability ( $\Lambda_{1.4}$ ) lies within the constraint ( $\Lambda_{1.4} \leq 800$ ) for GW170817 event [71]. But value of  $\Lambda_{1.4}$  obtained for DBHP model (682) has marginal overlap with revised limit  $\Lambda_{1.4} \leq 580$  within  $1\sigma$  uncertainty [18]. This is attributed to the impact of inclusion of PREX-II data in our fit which produces stiff symmetry energy with density slope  $L = 83.9$  MeV. We are looking forward that the new terrestrial experiments and astrophysical observations may impose tighter bounds.

In Table IV, we present the results for the various properties of static stars with DBHP parameterization. The theoretical uncertainties calculated for the properties using Eqs. (13 and 14) are also listed. Results obtained with other parameter sets are also shown for compari-

son. We obtain a very small theoretical uncertainties for the maximum mass  $M_{max}$  (1.9 %), maximum mass radius  $R_{max}$  (2.5 %) and radius  $R_{1.4}$  (3 %) of neutron star. The small uncertainties might be attributed to the fact that the inclusion of  $M_{max}$  in the fit data constraint the high density regime of EOS. A relatively large uncertainties ( $\approx 18$  %) is obtained for  $\Lambda_{1.4}$ . This is due to the fact that  $\Lambda \propto R^5$  which indicates that precise measurement of tidal deformability can constrain the NS radius in narrow bounds. Indeed it is believed that no terrestrial experiment can reliably constrain the EOS of neutron star [3].

### C. Correlations of nuclear matter, neutron star properties and model parameters

We now discuss the correlation coefficients, shown in Fig. 9, between the model parameters and nuclear matter properties, neutron skin thickness of  $^{208}\text{Pb}$  nucleus as well as NS observables. The isoscalar nuclear matter properties like  $E/A$ ,  $K$ ,  $M^*/M$  show strong correlations with isoscalar parameters  $g_{\sigma}$ ,  $g_{\omega}$  and  $\bar{\kappa}$ . It can also be observed from the figure that the symmetry energy slope parameter ( $L$ ) can be constrained by the coupling parameter  $a_2$ ,  $b_1$  and  $b_2$  along with the coupling parameter  $g_{\rho}$  as suggested by their correlations. The value of  $\Delta r_{np}$  is found to be well constrained by the parameters  $g_{\rho}$  and  $b_2$  as they have strong correlations. This study is quite consistent with results reported in [33, 35]. Finally, we discuss the correlations between neutron star observables and Lagrangian model parameters as shown in Fig. 9. A strong correlation between maximum neutron star mass and  $\omega$ -meson self-coupling parameter  $\zeta$  is missing in case of DBHP model parameterization. The  $M_{max}$  display a moderate correlations with isovector coupling parameter  $c_1$  and  $b_1$ . A large maximum mass may be generated either by having a stiff EOS for SNM or a stiff symmetry energy. If the symmetry energy is soft, then one must stiffen EOS of SNM which can be done by tuning the parameter  $\zeta$ . But the symmetry energy of DBHP model is stiff as shown by the Fig. 5. The symmetry energy slope parameter at saturation density is found to be 83.9 MeV. The stiff symmetry energy thereby weakens the correlation between  $\zeta$  and  $M_{max}$ . This suggests that the maximum mass results from a competition between  $\zeta$  and  $L$ . This further implies that the parameter

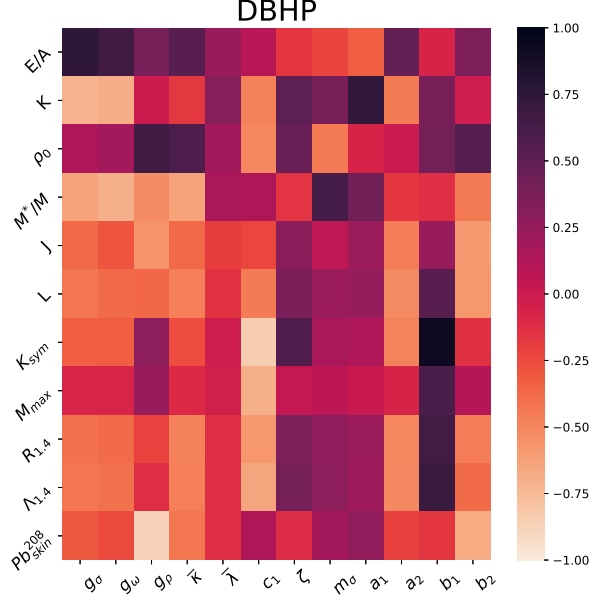


FIG. 9. (Color online) Correlation coefficients between the model parameters and a set of neutron star observables as well as the bulk properties of nuclear matter at the saturation density for DBHP parametrization (see text for details).

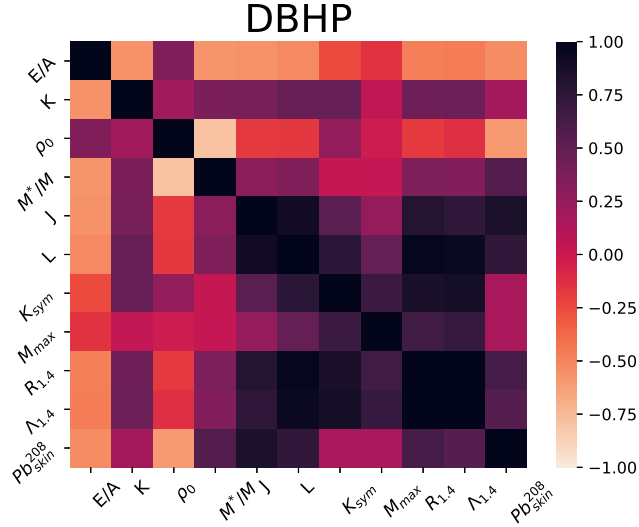


FIG. 10. (Color online) Correlation coefficients for bulk nuclear matter and neutron star properties and neutron skin of  $^{208}\text{Pb}$  for DBHP parametrization.

$\zeta$  should be well correlated to  $c_1$  and  $b_1$  and this is what exactly reflected from the correlations shown in Fig.1. The values of  $L$  and  $K_{sym}$  are found to be constrained by the parameters  $c_1$  and  $b_1$ . Finally, in Fig. 10 we display the correlation coefficients between the properties of nuclear matter, neutron star, and neutron skin thickness of  $^{208}\text{Pb}$ . A strong correlation of neutron skin thickness of  $^{208}\text{Pb}$  nucleus with  $J$ ,  $L$ ,  $R_{1.4}$  and  $\Lambda_{1.4}$  is observed. As per the expectation, radius  $R_{1.4}$  is found to have a strong

correlation with  $J$  and  $L$ . These findings are quite in harmony with the results reported in Ref. [33, 35]. The curvature of the symmetry energy ( $K_{sym}$ ) is also found to have a strong correlation with  $R_{1.4}$  and  $\Lambda_{1.4}$ .

## V. SUMMARY

The new relativistic interaction DBHP for the relativistic mean field model has been generated by keeping in view the PREX-II data for neutron-skin in  $^{208}\text{Pb}$  nucleus, astrophysical constraints in addition to those usually employed, like, binding energy, charge radii for finite nuclei and empirical data on nuclear matter at the saturation density. We have included all possible self and mixed interactions between  $\sigma$ ,  $\omega$ , and  $\rho$ -meson up to the quartic order so that the coupling parameters obey the naturalness behavior as imposed by the effective field theory [28]. The Covariance analysis enabled us to assess the statistical uncertainties in the estimation of the model parameters and observables of interest as well as the correlations among them. The DBHP parameter set is obtained such that it reproduces the ground state properties of the finite nuclei, bulk nuclear matter properties and also satisfies the constraints of mass and radius of the neutron star and its dimensionless deformability  $\Lambda$  from recent astrophysical observations [18, 19, 58, 66]. The root mean square errors in the total binding energies and charge rms radii for finite nuclei included in our fit for DBHP parameterization are 2.1 MeV and 0.02 fm respectively.

The Bulk nuclear matter properties obtained are well consistent with the current empirical data [3, 57]. The maximum gravitational mass and radius ( $R_{1.4}$ ) of the neutron star comes out to be  $2.029 \pm 0.038 M_{\odot}$  and  $13.388 \pm 0.521$  km respectively [41]. The value of  $\Lambda_{1.4}$  which is equal to  $682.497 \pm 125.090$  for DBHP parameterization also satisfies the constraints for GW170817 event [71] and reported in Refs. [3, 72]. The parametrization generated in consideration of PREX-II data produces stiff symmetry energy coefficient and its density dependence leading to the  $\Lambda_{1.4} = 682 \pm 125$  which has marginal overlap with the revised constraint [18]. We are looking forward that the new terrestrial experiments and astrophysical observations may put more stringent constraints on the density dependence of the symmetry energy.

## ACKNOWLEDGMENTS

V.T. is highly thankful to Himachal Pradesh University for providing computational facility and the Department of Science & Technology (Govt. of India) for providing financial assistance (DST/INSPIRE Fellowship/2017/IF170302) under Junior/Senior Research Fellowship scheme. C.M. acknowledges partial support from the IN2P3 Master Project “NewMAC”.

- 
- [1] J. M. Lattimer and M. Prakash. *Science*, 304:536, 2004.
  - [2] C. J. Horowitz and J. Piekarewicz. Neutron star structure and the neutron radius of 208pb. *Phys. Rev. Lett.*, 86:5647–5650, 2001.
  - [3] Brendan T Reed, Farrukh J Fattoyev, Charles J Horowitz, and Jorge Piekarewicz. Implications of prex-2 on the equation of state of neutron-rich matter. *Physical Review Letters*, 126(17):172503, 2021.
  - [4] F. J. Fattoyev, J. Piekarewicz, and C. J. Horowitz. Neutron skins and neutron stars in the multimessenger era. *Phys. Rev. Lett.*, 120:172702, Apr 2018.
  - [5] Shashi K Dhiman, Raj Kumar, and B. K. Agrawal. Non-rotating and rotating neutron stars in the extended field theoretical model. *Phys. Rev. C*, 76(4):045801, 2007.
  - [6] Bikram Keshari Pradhan, Debarati Chatterjee, Radhika Gandhi, and Jürgen Schaffner-Bielich. Role of vector self-interaction in neutron star properties. *Nuclear Physics A*, page 122578, 2022.
  - [7] Virender Thakur, Raj Kumar, Pankaj Kumar, Vikesh Kumar, BK Agrawal, and Shashi K Dhiman. Relativistic mean field model parametrizations in the light of gw170817, gw190814, and psr j 0740+ 6620. *Physical Review C*, 106(2):025803, 2022.
  - [8] Virender Thakur, Raj Kumar, Pankaj Kumar, Vikesh Kumar, Mukul Kumar, C Mondal, BK Agrawal, and Shashi K Dhiman. Effects of an isovector scalar meson on the equation of state of dense matter within a relativistic mean field model. *Physical Review C*, 106(4):045806, 2022.
  - [9] Suman Thakur, Virender Thakur, Raj Kumar, and Shashi K Dhiman. Structural properties of rotating hybrid compact stars with color-flavor-locked quark matter core and their tidal deformability. *The European Physical Journal A*, 58(5):1–22, 2022.
  - [10] Paweł Haensel, Aleksander Yu Potekhin, and Dmitry G Yakovlev. *Neutron stars 1: Equation of state and structure*, volume 326. Springer Science & Business Media, 2007.
  - [11] J. M. Lattimer. Neutron stars. *Gen. Rel. Grav.*, 46:1713, 2014.
  - [12] G. Baym, T. Hatsuda, T. Kojo, P. D. Powell, Y. Song, and T. Takatsuka. From hadrons to quarks in neutron stars: a review. *Rep. Prog. Phys.*, 81:056902, 2018.
  - [13] K. Hebeler, J. M. Lattimer, C. J. Pethick, and A. Schwenk. Constraints on neutron star radii based on chiral effective field theory interactions. *Phys. Rev. Lett.*, 105:161102, Oct 2010.
  - [14] K Hebeler, JM Lattimer, Christopher J Pethick, and A Schwenk. Equation of state and neutron star properties constrained by nuclear physics and observation. *The Astrophysical Journal*, 773(1):11, 2013.
  - [15] James M Lattimer. The nuclear equation of state and neutron star masses. *Annu. Rev. Nucl. Part. Sci.*, 62:485–515, 2012.
  - [16] P. B. Demorest, Tim Pennucci, S. M. Ransom, M. S. E. Roberts, and J. W. T. Hessels. A two-solar-mass neutron star measured using Shapiro delay. *nature*, 467(7319):1081, 2010.
  - [17] John Antoniadis, Paulo C. C. Freire, Norbert Wex, Thomas M Tauris, Ryan S Lynch, Marten H van Kerkwijk, Michael Kramer, Cees Bassa, Vik S Dhillon, Thomas Driebe, et al. A massive pulsar in a compact

- relativistic binary. *Science*, 340(6131):1233232, 2013.
- [18] B. P. Abbott, R. Abbott, T. D. Abbott, F. Acernese, K. Ackley, C. Adams, T. Adams, P. Addesso, R. X. Adhikari, V. B. Adya, et al. Gw170817: Measurements of neutron star radii and equation of state. *Phys. Rev. Lett.*, 121(16):161101, 2018.
- [19] B. P. Abbott, R. Abbott, T. D. Abbott, F. Acernese, K. Ackley, C. Adams, T. Adams, P. Addesso, R. X. Adhikari, V. B. Adya, et al. Properties of the binary neutron star merger gw170817. *Phys. Rev. X*, 9(1):011001, 2019.
- [20] Zaven Arzoumanian, Adam Brazier, Sarah Burke-Spolaor, Sydney Chamberlin, Shami Chatterjee, Brian Christy, James M Cordes, Neil J Cornish, Fronefield Crawford, H Thankful Cromartie, et al. The nanograv 11-year data set: high-precision timing of 45 millisecond pulsars. *Astrophys. J. Suppl. S.*, 235(2):37, 2018.
- [21] M. C. Miller, F. K. Lamb, A. J. Dittmann, S. Bogdanov, Z. Arzoumanian, K. C. Gendreau, S. Guillot, A. K. Harding, W. C. G. Ho, J. M. Lattimer, R. M. Ludlam, S. Mahmoodifar, S. M. Morsink, P. S. Ray, T. E. Strohmayer, K. S. Wood, T. Enoto, R. Foster, T. Okajima, G. Prigozhin, and Y. Soong. PSR j0030+0451 mass and radius from NICER data and implications for the properties of neutron star matter. *The Astrophysical Journal*, 887(1):L24, dec 2019.
- [22] T. E. Riley, A. L. Watts, S. Bogdanov, P. S. Ray, R. M. Ludlam, S. Guillot, Z. Arzoumanian, C. L. Baker, A. V. Bilous, D. Chakrabarty, K. C. Gendreau, A. K. Harding, W. C. G. Ho, J. M. Lattimer, S. M. Morsink, and T. E. Strohmayer. A NICER view of PSR j0030+0451: Millisecond pulsar parameter estimation. 887:L21, 2019.
- [23] G. Raaijmakers, T. E. Riley, A. L. Watts, S. K. Greif, S. M. Morsink, K. Hebeler, A. Schwenk, T. Hinderer, S. Nissanke, S. Guillot, Z. Arzoumanian, S. Bogdanov, D. Chakrabarty, K. C. Gendreau, W. C. G. Ho, J. M. Lattimer, R. M. Ludlam, and M. T. Wolff. A NICER view of PSR j0030+0451: Implications for the dense matter equation of state. *The Astrophysical Journal*, 887:L22, 2019.
- [24] D Adhikari, H Albatineh, D Androic, K Aniol, DS Armstrong, T Averett, C Ayerbe Gayoso, S Barcus, V Bellini, RS Beminiwattha, et al. Accurate determination of the neutron skin thickness of pb 208 through parity-violation in electron scattering. *Physical review letters*, 126(17):172502, 2021.
- [25] J. M. Lattimer and M Prakash. Neutron star structure and the equation of state. *Astrophys. J.*, 550(1):426, 2001.
- [26] Roger W Romani, D Kandel, Alexei V Filippenko, Thomas G Brink, and WeiKang Zheng. Psr j0952- 0607: The fastest and heaviest known galactic neutron star. *The Astrophysical Journal Letters*, 934(2):L18, 2022.
- [27] P. Danielewicz. *Science*, 298:1592, 2002.
- [28] RJ Furnstahl, Brian D Serot, and Hua-Bin Tang. A chiral effective lagrangian for nuclei. *Nucl. Phys. A*, 615(4):441–482, 1997.
- [29] Raj Kumar, B. K. Agrawal, and Shashi K. Dhiman. Effects of  $\omega$  meson self-coupling on the properties of finite nuclei and neutron stars. *Phys. Rev. C*, 74:034323, Sep 2006.
- [30] TJ Bürvenich, DG Madland, and P-G Reinhard. Adjustment studies in self-consistent relativistic mean-field models. *Nuclear Physics A*, 744:92–107, 2004.
- [31] Scott Kirkpatrick. Optimization by simulated annealing: Quantitative studies. *Journal of statistical physics*, 34(5):975–986, 1984.
- [32] J Dobaczewski, W Nazarewicz, and PG Reinhard. Error estimates of theoretical models: a guide. *Journal of Physics G: Nuclear and Particle Physics*, 41(7):074001, 2014.
- [33] Wei-Chia Chen and Jorge Piekarewicz. Searching for isovector signatures in the neutron-rich oxygen and calcium isotopes. *Physics Letters B*, 748:284–288, 2015.
- [34] C Mondal, BK Agrawal, and JN De. Constraining the symmetry energy content of nuclear matter from nuclear masses: A covariance analysis. *Physical Review C*, 92(2):024302, 2015.
- [35] F. J. Fattoyev, C. J. Horowitz, J. Piekarewicz, and Brendan Reed. Gw190814: Impact of a 2.6 solar mass neutron star on the nucleonic equations of state. *Phys. Rev. C*, 102:065805, Dec 2020.
- [36] Siegmund Brandt. *Statistical and computational methods in data analysis*. Springer, 1997.
- [37] P.-G. Reinhard and W. Nazarewicz. Information content of a new observable: The case of the nuclear neutron skin. *Phys. Rev. C*, 81:051303, 2010.
- [38] Meng Wang, G Audi, FG Kondev, WJ Huang, S Naimi, and Xing Xu. The ame2016 atomic mass evaluation. *Chin. Phys. C*, 41:030003, 2017.
- [39] EW Otten. Treatise on heavy-ion science. *DA Bromley (ed.)*, 8:517, 1989.
- [40] H Vries, CW Jager, and C Vries. Atomic data and nuclear data table. 1987.
- [41] Luciano Rezzolla, Elias R. Most, and Lukas R. Weih. Using gravitational-wave observations and quasi-universal relations to constrain the maximum mass of neutron stars. *Astrophys. J. Lett.*, 852(2):L25, 2018.
- [42] Peter Ring and Peter Schuck. *The nuclear many-body problem*. Springer Science & Business Media, 1980.
- [43] S Karatzikos, AV Afanasjev, GA Lalazissis, and P Ring. The fission barriers in actinides and superheavy nuclei in covariant density functional theory. *Physics Letters B*, 689(2-3):72–81, 2010.
- [44] Meng Wang, WJ Huang, Filip G Kondev, Georges Audi, and Sarah Naimi. The ame 2020 atomic mass evaluation (ii). tables, graphs and references. *Chinese Physics C*, 45(3):030003, 2021.
- [45] GA Lalazissis, J König, and P Ring. New parametrization for the lagrangian density of relativistic mean field theory. *Physical Review C*, 55(1):540, 1997.
- [46] Bharat Kumar, S. K. Patra, and B. K. Agrawal. New relativistic effective interaction for finite nuclei, infinite nuclear matter, and neutron stars. *Phys. Rev. C*, 97:045806, Apr 2018.
- [47] F. J. Fattoyev, C. J. Horowitz, J. Piekarewicz, and Brendan Reed. Gw190814: Impact of a 2.6 solar mass neutron star on the nucleonic equations of state. *Phys. Rev. C*, 102:065805, Dec 2020.
- [48] Meng Wang, G Audi, FG Kondev, WJ Huang, S Naimi, and Xing Xu. The ame2016 atomic mass evaluation. *Chin. Phys. C*, 41:030003, 2017.
- [49] William G. Newton and Gabriel Crocombe. Nuclear symmetry energy from neutron skins and pure neutron matter in a bayesian framework. *Phys. Rev. C*, 103:064323, Jun 2021.
- [50] Jun Xu and Panagiota Papakonstantinou. Bayesian inference of finite-nuclei observables based on the kids model.

- Phys. Rev. C*, 105:044305, Apr 2022.
- [51] Hana Gil, Panagiota Papakonstantinou, and Chang Ho Hyun. Constraints on the curvature of nuclear symmetry energy from recent astronomical data within the kids framework. *International Journal of Modern Physics E*, 31(01):2250013, 2022.
- [52] D. Adhikari and et al. *arXiv:2205.11593*, 2022.
- [53] Esra Yuksel and Nils Paar. Implications of parity-violating electron scattering experiments on  $^{48}\text{Ca}$  (crex) and  $^{208}\text{Pb}$  (prex-ii) for nuclear energy density functionals. *arXiv preprint arXiv:2206.06527*, 2022.
- [54] Paul-Gerhard Reinhard, Xavier Roca-Maza, and Witold Nazarewicz. Combined theoretical analysis of the parity-violating asymmetry for  $^{48}\text{Ca}$  and  $^{208}\text{Pb}$ . *arXiv:2206.03134v1*, 2022.
- [55] Jorge Piekarewicz. Nuclear physics of neutron stars. 1128(1):144–153, 2009.
- [56] G Colo, U Garg, and H Sagawa. Symmetry energy from the nuclear collective motion: constraints from dipole, quadrupole, monopole and spin-dipole resonances. *The European Physical Journal A*, 50(2):1–12, 2014.
- [57] J Piekarewicz. Symmetry energy constraints from giant resonances: A relativistic mean-field theory overview. *The European Physical Journal A*, 50(2):1–18, 2014.
- [58] AW Steiner, JM Lattimer, and EF Brown. The equation of state from observed masses and radii of neutron stars *astrophys. J*, 722:33–54, 2010.
- [59] Thomas E Riley, Anna L Watts, Paul S Ray, Slavko Bogdanov, Sebastien Guillot, Sharon M Morsink, Anna V Bilous, Zaven Arzoumanian, Devarshi Choudhury, Julia S Deneva, et al. A nicer view of the massive pulsar psr j0740+ 6620 informed by radio timing and xmm-newton spectroscopy. *The Astrophysical Journal Letters*, 918(2):L27, 2021.
- [60] MC Miller, FK Lamb, AJ Dittmann, S Bogdanov, Z Arzoumanian, KC Gendreau, S Guillot, WCG Ho, JM Lattimer, M Loewenstein, et al. The radius of psr j0740+ 6620 from nicer and xmm-newton data. *arXiv preprint arXiv:2105.06979*, 2021.
- [61] J. R. Oppenheimer and G. M. Volkoff. On massive neutron cores. *Phys. Rev.*, 55:374–381, Feb 1939.
- [62] Richard C. Tolman. Static solutions of einstein’s field equations for spheres of fluid. *Phys. Rev.*, 55:364–373, Feb 1939.
- [63] Y Sugahara and H Toki. Relativistic mean-field theory for unstable nuclei with non-linear  $\sigma$  and  $\omega$  terms. *Nucl. Phys. A*, 579(3-4):557–572, 1994.
- [64] Emmanuel Fonseca, Timothy T Pennucci, Justin A Ellis, Ingrid H Stairs, David J Nice, Scott M Ransom, Paul B Demorest, Zaven Arzoumanian, Kathryn Crowter, Timothy Dolch, et al. The nanograv nine-year data set: Mass and geometric measurements of binary millisecond pulsars. *Astrophys. J.*, 832(2):167, 2016.
- [65] Eemeli Annala, Tyler Gorda, Alekski Kurkela, and Alekski Vuorinen. Gravitational-wave constraints on the neutron-star-matter equation of state. *Phys. Rev. Lett.*, 120:172703, Apr 2018.
- [66] Eemeli Annala, Tyler Gorda, Alekski Kurkela, and Alekski Vuorinen. Gravitational-wave constraints on the neutron-star-matter equation of state. *Physical review letters*, 120(17):172703, 2018.
- [67] Tanja Hinderer. Tidal love numbers of neutron stars. *Astrophys. J.*, 677(2):1216, 2008.
- [68] Tanja Hinderer, Benjamin D Lackey, Ryan N Lang, and Jocelyn S Read. Tidal deformability of neutron stars with realistic equations of state and their gravitational wave signatures in binary inspiral. *Phys. Rev. D*, 81(12):123016, 2010.
- [69] Tanja Hinderer. Erratum: “tidal love numbers of neutron stars” (2008, apj, 677, 1216). *Astrophys. J.*, 697(1):964, 2009.
- [70] Thibault Damour and Alessandro Nagar. Effective one body description of tidal effects in inspiralling compact binaries. *Phys. Rev. D.*, 81(8):084016, 2010.
- [71] Benjamin P Abbott, Rich Abbott, T. D. Abbott, Fausto Acernese, Kendall Ackley, Carl Adams, Thomas Adams, Paolo Addesso, R. X. Adhikari, V. B. Adya, et al. Gw170817: observation of gravitational waves from a binary neutron star inspiral. *Phys. Rev. Lett.*, 119(16):161101, 2017.
- [72] Yuxi Li, Houyuan Chen, Dehua Wen, and Jing Zhang. Constraining the nuclear symmetry energy and properties of the neutron star from gw170817 by bayesian analysis. *The European Physical Journal A*, 57(1):1–10, 2021.

